Physica 127B (1984) 37–45
North-Holland, Amsterdam

# SCANNING TUNNELING MICROSCOPY

G. BINNIG and H. ROHRER
*IBM Zurich Research Laboratory, 8803 Rüschlikon, Switzerland*

An overview of the status of Scanning Tunneling Microscopy (STM) is given. So far, the method has been applied mainly to surface structures. Examples are given for reconstructions on metal and semiconductor surfaces and adsorbate structures. It will become evident that the technique is likewise applicable to chemical investigations of surfaces on an atomic scale.

## 1. Introduction

Scanning Tunneling Microscopy (STM) has now left its infancy stage. The method is changing from an art to a technique, and theory from experimentalists' wishful thinking to fundamental understanding. Yet, there is still ample room for substantial progress in technique and theory. In the present article, we illustrate the status of the method with some recent experiments. The state of the theory is discussed in three separate papers of this volume [1].

The underlying physical principle of the method is the tunnel effect. Owing to their wave nature, the electrons, say in a metal, are not strictly confined to the interior bounded by the surface atoms. Therefore, the electron density does not drop to zero at the 'surface', but decays exponentially in the outside, however, with a short decay length of some ångströms [see fig. 1a]. This decay length is a measure of the potential barrier height the electrons experience outside the 'surface'. (The 'surface' is thus a much fuzzier interface for electrons than for atoms. In the following, the surface is defined as the outmost atom positions.) If two metals are approached to within a few Å, the overlap of their surrounding electron clouds becomes substantial, and a measurable current can be induced by applying a small voltage between them. This tunnel current, $J$, is thus a measure of the wave-function overlap, and depends very strongly on the distance between the two metals $s$ (~ a factor of ten per Å) and an average inverse decay length $\kappa_0$:

$$J \propto \exp(-A\kappa_0 s). \tag{1}$$

For two uniform metal surfaces, $\kappa_0 \approx \sqrt{1/2(\phi_1 + \phi_2)}$, where $\phi_1$ and $\phi_2$ are the respective work functions. $\kappa_0$ also denotes the average tunnel barrier height.

This extremely strong dependence on distance *and* decay length is the basis of the Scanning Tunneling Microscope. Descriptions of the technical realization are given in refs. 2–5. In short, one of the electrodes is sharpened to a pointed tip which is scanned over the surface to be investigated (the other electrode) at constant tunnel current (see fig. 1). The tip thus traces contours of constant wave-function overlap. Only in the case of constant decay length, are the traces an almost true image of the surface atomic positions, i.e., the surface topography. Generally, an STM graph will reflect at least qualitatively the surface topography in the case of clean metal surfaces, for many other surfaces it is not necessarily so.

This might be considered a drawback of the method. We believe, however, that it is more than offset by the wealth of information obtained on the electronic properties. In addition, the method is even energy selective (only the electrons lying within the energy window Fermi energy ± applied voltage contribute to the tunneling) and spin selective (this in the case of a polarized tip). Thus, STM is not simply a surface structural method, but also, say, a surface chemical method with the same atomic resolution.

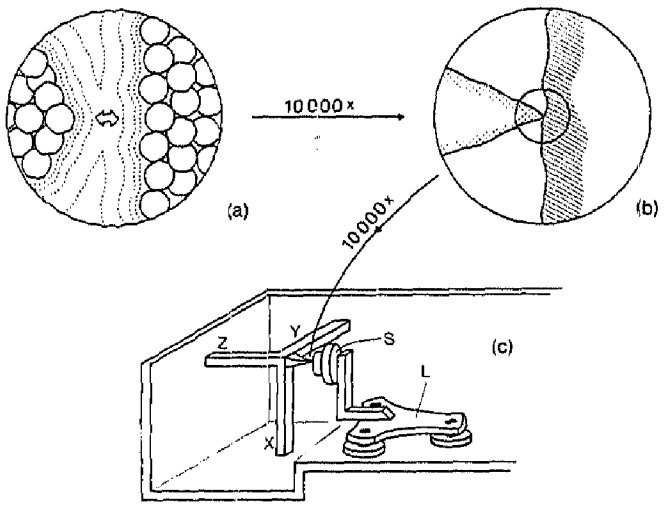


Fig. 1. Schematic of the physical principle and technical realization of STM. (a) shows apex of the tip (left) and surface (right) at a magnification of about $10^8$. The solid circles indicate atoms, the dotted lines electron density contours. The path of the tunnel current is given by the arrow. (b) Scaled down by a factor of $10^4$. The tip (left) appears touching the surface (right). (c) STM with rectangular piezo drive X, Y, Z of the tunnel tip (length of each leg about 5 cm) at left and 'louse' L (electrostatic 'motor') for rough positioning ($\mu$m to cm range) of sample S.

which at present reaches 0.05 Å vertically and 2 Å laterally. The vertical resolution is a matter of mechanical stability, the lateral one is given by the width of the 'tunnel channel'. Experimentally, the lateral resolution is better than expected from theoretical considerations [6–9]. This is partly attributed to focussing of the tunnel current (in addition to the geometrical one) by local lowering of the tunnel barrier height at the apex of the tip and/or tunneling into or out of localized tip wave functions [10]. Before turning to a few specific examples, we list some important and partly unique characteristics of STM:

1) It gives 3-D images of surfaces direct in real space and on an atomic scale *in all three* dimensions.

2) It employs only bound particles and no lenses (the only other real-space, lens-less method is field ion microscopy, FIM).

3) It is nondestructive. Electron energies and electric fields on the surface lie in the mV and $10^4$ V/cm range, respectively, (typical values used at present, but, in principle, there are no difficulties in going to considerably lower energies and fields and, if desired, also to higher ones).

4) It is a structural *and* and chemical method, applicable to both periodic and nonperiodic surface features.

5) It can also be operated at ambient pressure (with some loss in resolution) and eventually in liquids.

These attractive properties have obviously intrigued many scientists. Gone beyond contemplation were, to our knowledge, Young, and coworkers [11] and Thompson and Hanrahan [12]. However, mainly stability problems prevented operation as Scanning Tunneling Microscopes.

Systematic experiments have so far dealt mainly with structural aspects of and on surfaces, i.e., images were taken at fixed tunnel current

and voltage. However, exploratory mapping of the local decay length with the modulation technique [3–5] could be obtained with a resolution comparable to constant-current STM graphs [5]. In the following, we present three recent examples obtained on a clean metal surface, semiconductor surface and an adsorbate structure on a metal, respectively.

## 2. STM on clean metal surfaces

For clean metal surfaces, one expects that an STM graph, taken at constant tunnel current and voltage, reflects at least qualitatively the surface topography. Indeed, satisfactory agreement between experiments on Au(110) and the newly developed approaches for local tunneling was obtained [6, 7], although variations of the local tunnel barrier height (local decay length) have not been taken into account. An appreciable local polarization is induced by the corrugation itself even on clean metal surfaces, which can lead to strong variations of the local tunnel barrier *and* an overall reduction of the work function (≈ square of the inverse decay length) [13, 14]. The main result of the STM investigations of the Au(110) surface was the (111) facetting of the whole surface as the basic driving mechanism for the reconstructions and their disorder [15]. This established the missing-row model for the $1\times2$ reconstruction.

The Au(100) surface shows a rather large unit cell with an underlying dominant $1\times5$ corrugation. The STM experiments [16] are consistent in all respects with the reconstruction being formed by an incommensurate hexagonal top layer on the cubic second layer. Fig. 2 shows two STM graphs exhibiting the large, slightly irregular pseudo unit cell [in fig. 2(b), the reconstruction extends over a [011] step line]. The hexagonal layer is contracted by 3.82% and rotated by 0.1 degree. It should be noted that, in general, STM provides the principal structural features with usually less accuracy on the atomic position than other surface-sensitive methods like LEED. The rather accurate structural parameters in the present case are a consequence of the extreme sensitivity of the interference pattern between top and second layers to small structural changes. Other important and interesting observations and conclusions concern: a) The reconstruction nucleates at step lines. The latter, however, are not simply nucleation lines for the reconstruction, but are also modified by it (meandering [011] step line). b) (Carbon) contaminants are seen atom by atom. c) Carbon contaminations cluster on the surface. Even on appreciably contaminated surfaces, lakes of fully developed reconstructions appear, surrounded by carbon clusters. d) The reconstruction shows all the details already in the immediate vicinity of carbon clusters. The edges of the latter appear to run predominantly along the [011] and [01$\bar{1}$] directions.

## 3. STM on semiconductor surfaces

From the experimental point of view, semiconductor surfaces do not cause any new problems, even at quite high resistivities [17, 18]. Our shining example is the $7\times7$ reconstruction of the Si(111) surface [18]. Although contact between STM experiments and the surface structure is more involved, STM yielded a set of structural features which ruled out all the structures hitherto proposed, except the Harrison adatom model [19]. However, some questions remained open: (a) The high voltage of 2.8 V, which had to be applied in the 100 Ω cm, n-type silicon sample was not understood. (2) The contamination state of the sample was not checked by an independent method, and the reconstruction was only observed on lakes surrounded by a hilly structure of unidentified nature. (3) A threefold rotational symmetry of the reconstruction was proposed on the basis of some qualitative corrections for recorder overshoot. Recent experiments [20] with 1 Ω cm, p-type boron-doped silicon could be performed at low voltages. This indicates bulk-limited tunneling in the previous, high ohmic sample [21]. A contour plot of the new experiments is shown in fig. 3. The $7\times7$ reconstruction was generated by annealing at 1200 °C without sputter cleaning. No contamination was detected by AES analysis, a good LEED picture

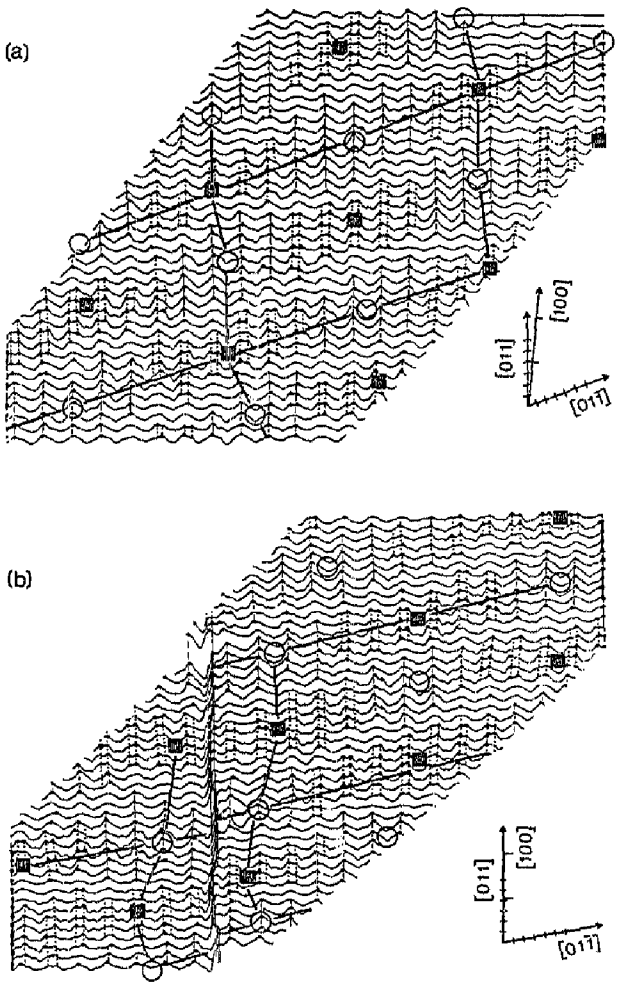


Fig. 2. High-resolution micrographs of Au(100) showing large pseudo unit cells indicated by the broken lines. (b) contains a meandering step line running in the [001] direction. The dots on the scans locate maxima with a curvature above a certain threshold. The alternating sequences of double-maxima, double-minima and single-maxima, single-minima structures in the [011] direction with ribbons of smooth corrugation in between are clearly evident. The lines connecting maxima are drawn by eye for better visibility of the two typical local $1\times5$ structures forming the large pseudo unit cell. Shearing of the latter in the $[01\bar{1}]$ direction is also clearly visible. Divisions on the axes correspond to 5 Å.

Fig. 3. Top view contours of the 7×7 reconstruction of boron doped silicon. The contours of equal height are spaced 0.2 Å apart, the brightness scale goes from white for maxima to gray for minima. The broken lines indicate the 7×7 unit cells. In the upper right corner, a maximum is missing.

was observed and no instrumental corrections had to be applied. The structural features are essentially the same as before: deep corner minima, less deep but still pronounced edge minima and twelve maxima. The maxima in the right half of the $7\times7$ unit cell are higher than in the left half, the three highest ones lying adjacent to the corner minima. If the instrumental corrections necessary in the previous experiment are made quantitative [22], the two structures will be practically equivalent, except for the occasional missing maximum (see upper right in fig. 3). This is attributed to a surface boron which cannot accommodate whatever causes the maxima (although the occurrence of missing maxima is much more frequent than expected from the bulk boron concentration). The fact that the missing maximum does not noticeably affect the rest of the unit cell is taken as an indication that the maxima are indeed caused by structures sitting on top of the surface, e.g., adatoms or modified milkstool structures [23]. Recently, Demuth et al. [24] concluded from rare gas titration studies, that work function variations across the unit cell are small and that thus the corrugation observed by STM are mainly structurally derived.

Finally, note that also in this case the reconstruction is not affected by nearby large-scale surface defects such as in the original experiments the hilly structure surrounding the reconstructed areas.

## 4. Oxygen on Ni(110)

This experiment [25] was aimed at exploring the potential of STM for adsorbate structures. Besides, the $2\times1$ reconstruction of oxygen-covered nickel is still an interesting open problem.

Experience shows that adsorbates generally give rise to quite sharp STM structures [4, 16]. These were, however, single adsorbates or adsorbate clusters, and it is not a priori clear that STM does not drastically affect adsorbate structures in some unexpected way. The present experiments on an ordered adsorbate structure should be more conclusive in this respect. A clean Ni(110) surface was first prepared by conventional ion bombardment and annealing cycles. After an oxygen exposure in excess of 1L, the LEED picture changed to the characteristic $2\times1$ pattern. Fig. 4 shows a contour-line representation of an STM graph. The loss in resolution in the upper part is due to an inadvertent change in tip condition, coinciding with a narrow domain wall in the $[01\bar{1}]$ direction. In the following, we concentrate on the lower part of the figure. The distinct maxima form domains with $2\times1$ structures separated in the $[1\bar{1}0]$ direction by wide domain walls. The sharp maxima are associated [25] with the individual oxygen atoms, and the intervening flat regions with uncovered unreconstructed Ni(110) on which the long ridges represent the close-packed, bare Ni rows. This is a good example to point out the similarity to and difference between STM and TEAMS (Thermal Energy Atomic and Molecular Scattering). Both methods test in their way the electron density at some distance outside the surface. The distance in TEAMS and STM is given by the energy of the atomic beam and the tunnel current, respectively. But whereas in TEAMS, the interaction is determined by the total electron density outside the surface, only the states near the Fermi level (within the voltage across the tunneling gap) contribute in STM. This can lead to significant differences in the corrugation measured [26]. On clean Ni, TEAMS detects a measurable corrugation in both principal crystal directions, but does not give any structure due to oxygen. STM, on the other hand, only resolves the uncovered Ni rows (with a larger corrugation though) but clearly shows structure due to the chemisorbed oxygen.

The detailed shape of the corrugation measured and the registry in the [001] direction of the oxygen atoms with respect to the bare Ni rows and in the $[1\bar{1}0]$ direction with step lines, respectively, are consistent with a sawtooth model of the reconstructed Ni, with the oxygen atoms sitting in long bridge sites. The experiment also gives a clue to why the saturation coverage, $\theta$, of the saturated $2\times1$ structure is about 1/3 [27] instead of 1/2. Counting simply the number of

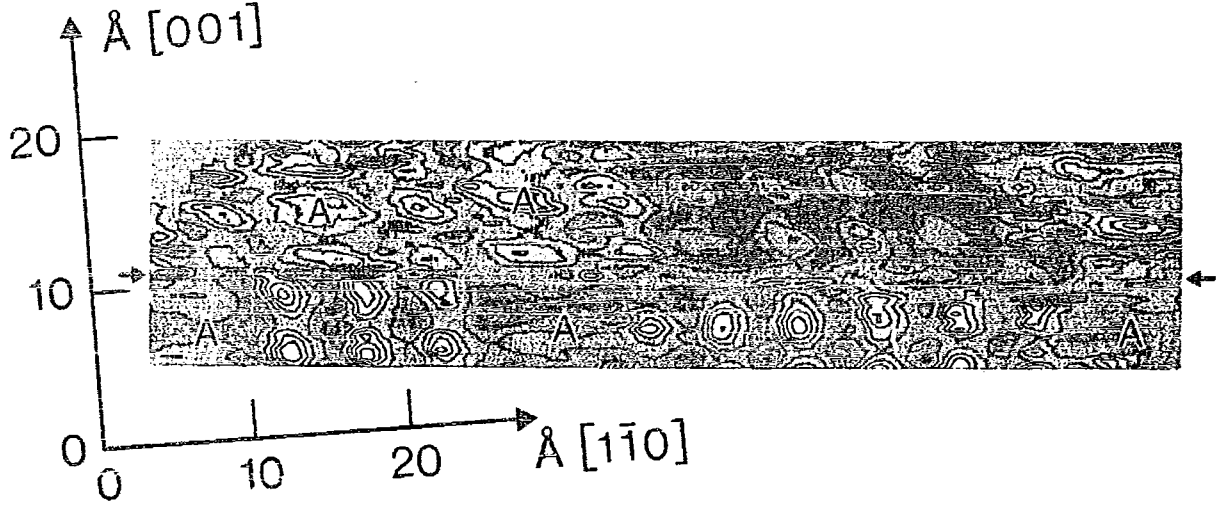


Fig. 4. Top view of STM graph of oxygen chemisorbed on Ni(110). The contours of equal corrugation height are spaced 0.1 Å apart in the lower, and 0.05 Å apart in the upper part. The brightness scale goes from white for maxima to gray for minima. The loss of resolution observed in the upper part marked by the arrows is due to an inadvertent change in the tip condition. The arrows also locate a narrow domain wall in the [1$\bar{1}$0] direction which might have induced that change. The regions of 2×1 structures are separated in the [1$\bar{1}$0] direction by wide domain walls (marked with A).

oxygen atoms, we always arrive at $\theta = 0.35$ for various surface regions. Responsible for the reduced saturation coverage are the uncovered parts which act as sort of domain walls running along the [001] direction between the $2\times1$ regions and are always $1\frac{1}{2}$ surface unit cells wide.

## 5. Conclusions

The above three examples establish STM as a surface structural method. Besides the resolution, a particularly appealing feature is the simultaneous observation of periodic and non-periodic structures. Very often this turns out to be of great help in determining both the correct surface structure and its registry on the bulk structure.

Compositional and chemical analysis of surfaces on an atomic scale is another area where we believe that STM will make decisive contributions. The experiment on oxygen covered Ni [25] is the first important step in this direction. In future investigations, decay-length mappings as well as local tunnel spectroscopy (e.g., $I$–$V$ characteristics) will be a central element. They contain the chemical information of the surface. An important result in this respect is a recent investigation [15] on the role of the image potential (for references on image potential in tunneling see ref. [15]). For tunnel barrier width of a few Å (generally used in STM), the image potential reduces substantially the tunnel barrier height. Thus, the actual decay length depends on the distance, s, between tunnel tip and electrode, and is therefore no longer an intrinsic surface electronic property. However, it was shown experimentally and theoretically [15], that the relative change of tunnel current with s is still mainly determined by the undisturbed barrier height, i.e., by an intrinsic surface property.

A third class of experiments will deal with special objects on a surface, which now acts as the 'sample holder'. Preliminary experiments on DNA on carbon look very promising [28]. Although no details have yet been resolved, the DNA's appear as long strands, both in the constant tunnel current, topographical approach as well as work function profiles.

There is of course, an abundance of further applications of STM in science and technology. We are convinced that with progress in method and understanding, many new interesting aspects will evolve. Just imagine, for instance, what could be done with a highly focussed beam (say with a diameter of 10 Å and upwards) of low-energy electrons (meV and upwards).

It is a pleasure to thank all our colleagues for their valuable support, advice and interest, in particular our two close collaborators, Ch. Gerber and E. Weibel.

## References

[1] N. Garcia; A. Baratoff; D. Hamann; all in this volume.
[2] G. Binnig, H. Rohrer, Ch. Gerber and E. Weibel, Appl. Phys. Lett. 40 (1982) 178.
[3] G. Binnig and H. Rohrer, Helv. Phys. Acta 55 (1982) 726.
[4] G. Binnig, H. Rohrer, Ch. Gerber and E. Weibel, Phys. Rev. Lett. 49 (1982) 57.
[5] G. Binnig and H. Rohrer, Surface Sci. 126 (1983) 236.
[6] J. Tersoff and D. Hamann, Phys. Rev. Lett. 50 (1983) 1998.
[7] N. Garcia, C. Ocal and F. Flores, Phys. Rev. Lett. 50 (1983) 2002.
[8] E. Stoll, Surface Sci. 143 (1984) L411.
[9] E. Stoll, A. Baratoff, A. Selloni and P. Carnevali, J. Phys. C 17 (1984) 3073.
[10] A. Baratoff, Condensed Matter Division, EPS 3rd General Conference, Abstracts 7b (1983) 864.
T.E. Geuchtwang, P.H. Cutler and N.M. Minkovsky, Physics Lett. 99A (1983) 167.
[11] R.D. Young, J. Ward and F. Scire, Phys. Rev. Lett. 27 (1971) 922; Rev. Sci. Instrum. 43 (1972) 999.
E.C. Teague, Bull. Am. Phys. Soc. 23 (1978) 290; Thesis, North Texas State University, Denton, Texas (1978).
[12] W. Thompson and S.F. Hanrahan, Rev. Sci. Instrum. 47 (1976) 1303.
[13] G. Binnig, H. Rohrer, Ch. Gerber and E. Weibel, Surface Sci. 131 (1983) L379.
[14] N.D. Lang, Solid State Physics 28 (1973) 278.
H. Ehrenreich, F. Seitz and D. Turnbull, eds. (Academic Press, New York, 1973).
[15] G. Binnig, N. Garcia, H. Rohrer, J.M. Soler and F. Flores, Phys. Rev. B (15 Sept., 1984, issue).
[16] G. Binnig and H. Rohrer, in: Proc. IX IVC-V ICSS, Madrid, 1983, to be published in J. Vacuum Sci. Technol. 1984.
G. Binnig, H. Rohrer, Ch. Gerber and E. Stoll, Surface Sci., 144 (1984) in press.

[17] H.J. Scheel, G. Binnig and H. Rohrer, J. Crystal Growth 60 (1982) 199.
[18] G. Binnig, H. Rohrer, Ch. Gerber and E. Weibel, Phys. Rev. Lett. 50 (1983) 120.
[19] W.A. Harrison, Surface Sci. 55 (1976) 1.
[20] G. Binnig, H. Rohrer, F. Salvan, Ch. Gerber and A. Baró, to be published.
[21] A. Baratoff, private communication. F. Flores and N. Garcia, to be published.
[22] H. Thomas and E. Stoll, IBM Research Report RZ 1304 (May 1984).
[23] L.C. Snyder, Surf. Sci. 140 (1984) 101; M. Aono, R. Souda, C. Oshima and Y. Ishizawa, Phys. Rev. Lett. 51 (1983) 801.
[24] J. Demuth and A.J. Scheil-Sorokin, to be published.
[25] A.M. Baró, G. Binnig, H. Rohrer, Ch. Gerber, E. Stoll, A. Baratoff and F. Salvan, Phys. Rev. Lett. 52 (1984) 1304.
[26] P.J. Feibelman and D.R. Hamann, Phys. Rev. Lett. 52 (1984) 61.
[27] R.G. Smeenk, R.M. Tromp, J.F. Van der Veen and F.W. Saris, Surface Sci. 95 (1980) 156; J.A. Van den Berg, L.K. Verheij and D.G. Armour, Surface Sci. 91 (1980) 218.
[28] Work performed in collaboration with the Institute of Cell Biology, Swiss Federal Institute of Technology, (ETH), Zurich.